

Experimental Study on Seismic Performance of Precast Reinforced Concrete Core Walls

T. Nakachi

Fukui University of Technology, Japan

R. Tokunaga

DKshiken Co., Ltd., Japan



SUMMARY:

Multistory core walls installed in high-rise reinforced concrete buildings effectively reduce seismic vibration. In high-rise buildings with the core wall system, which consists of four L-shaped core walls, the axial load of the core wall is remarkably high under the action of diagonal seismic force. On the other hand, precast core walls are considered effective in construction because they can be built more quickly than cast-in-place core walls. In this study, a lateral loading test was conducted on precast wall columns simulating the corner and the area near the corner of the L-shaped precast core wall. The specimen consisted of four square-section precast columns. The vertical joints between the precast columns were grouted with high-strength mortar. Each precast column had cotters at the vertical joint. Based on the results of the lateral loading tests, the seismic performance of wall columns was clarified.

Keywords: Reinforced concrete, core wall, precast, horizontal tied rebar, cotter

1. INTRODUCTION

In high-rise buildings with a core wall system, the axial load of the core wall is very high under the action of seismic force. In particular, the corner and the area near the corner of L-shaped core walls are subjected to high compressive stress and should be reinforced to improve the deformation capacity of core walls. Previously, we conducted lateral loading tests on multistory L-shaped reinforced concrete core walls and examined the relationship between the confinement effect of these areas and the deformation capacity of core walls.¹⁾ We also analyzed the results of the lateral loading tests using the three-dimensional nonlinear finite element method.²⁾ On the other hand, it is considered that precast core walls are effective in construction because they can be built more quickly than cast-in-place core walls. Regarding precast concrete multistory shear walls in high-rise buildings, Komiya et al. conducted lateral loading tests on wall columns having precast edge areas and examined their structural performance.³⁾ Nakazawa et al. also conducted lateral loading tests on core walls for which the edge areas were precast columns.⁴⁾ In this paper, a lateral loading test on full precast wall columns simulating the area near the corner of an L-shaped core wall was conducted in order to examine the seismic performance. The wall column was divided into precast columns, and the vertical joints between columns were grouted without cotter bars. Each precast column had cotters at the vertical joint. Horizontal tied rebars were concentrated at the second and third floor level to connect the precast columns.

2. SUMMARY OF TEST

2.1 Test Specimen

The configuration and arrangement of reinforcement in the specimen are shown in Fig. 1. The physical properties of the concrete and reinforcement are listed in Table 1 and Table 2, respectively. A

one-eighth-scale precast wall column specimen simulating the area near the corner of an L-shaped core wall was tested. The specimen represented the lower three stories of a high-rise building of approximately twenty-five stories. The specimen had a rectangular cross section measuring 90×405 mm, was the flexural type and had a shear span ratio of 2.4. The specimen consisted of four square-section precast columns arranged in a line. The width of the opening between columns was 7 mm, and the openings were grouted. Each precast column had cotters without cotter bars at the vertical joint, and the depth of the cotter was 6 mm. The specified design strength of the concrete was 60 N/mm², and that of the grout was 80 N/mm². The concrete for the second and third floor was cast after the vertical joints of the precast columns were grouted. The horizontal tied rebars were concentrated at the floor level to connect the precast columns. D10 deformation bars with yield strength of 397 N/mm² were used for the main bars of the precast columns and the horizontal tied rebars. High-strength bars U5.1 with yield strength of 1368 N/mm² were used for the hoops of the precast columns. Specimen cover concrete was 6 mm thick.

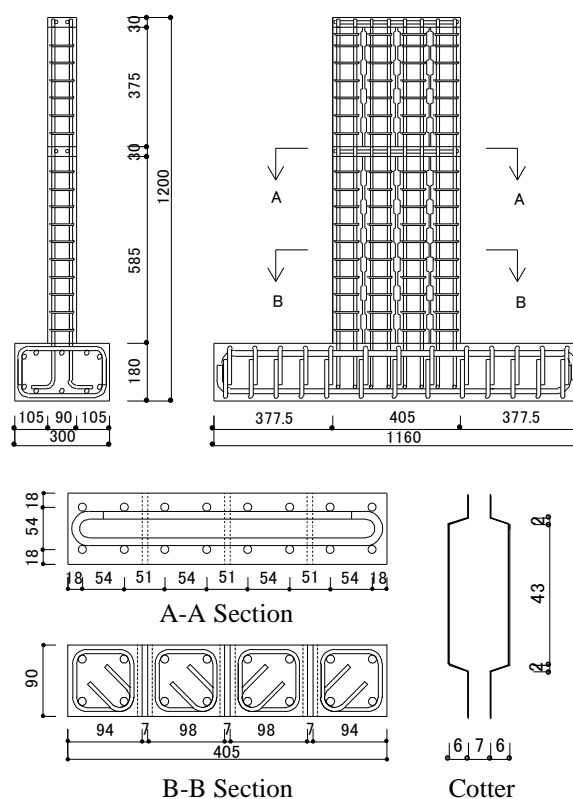


Fig. 1 Test Specimen

2.2 Test Procedure

The loading test was a cantilever type, as shown in Fig. 2. In the cyclic lateral loading test, the specimen was subjected to lateral forces by a horizontal hydraulic jack connected to the reaction frame. Positive loading was conducted by pulling the PC steel bars with the jack. The PC steel bars were attached to the pin support on the right side of the specimen (Fig. 2). Therefore, the specimen was pushed from the right side. Loading was conducted without tying the precast columns with the PC steel bars. Negative loading was conducted by pushing the specimen with the jack from the left side. A constant axial loading force was applied by a vertical hydraulic jack over the specimen to represent the axial stress in the stage of coupling beam yielding at the center core. The axial stress was 20% of the concrete compressive cylinder strength. Loading was controlled by the horizontal drift angle at a height corresponding to the second floor level (h : 615 mm). The loading was cyclic lateral loading at R (drift angle) = 1/1000 (rad.) (1 cycle), 2/1000, 5/1000, 7.5/1000, 10/1000, 15/1000, 20/1000 (2 cycle respectively), 30/1000 (1 cycle). The relative displacement was measured by displacement transducers, such as the expansion and contraction of each segment and the relative sliding and opening displacement in the vertical joints. Strain gages were attached to the hoop, the horizontal tied rebars and the main bars. The attachment position of strain gages at the hoop was the midpoint of the side.

Table 1 Physical Properties of Concrete

	Compressive Strength (N/mm ²)	Young's Modulus ($\times 10^4$ N/mm ²)	Split Strength (N/mm ²)
Precast	67.0	2.94	2.45
Latter	65.3	2.85	2.34
Grout	89.6	2.89	6.08

Table 2 Physical Properties of Steel

Bar Size	Yield Strength (N/mm ²)	Maximum Strength (N/mm ²)	Young's Modulus ($\times 10^5$ N/mm ²)	Elongation (%)
D10	397	577	1.85	18.5
U5.1	1368	1491	2.11	9.3

3. TEST RESULTS

3.1 Fracture Process

The crack patterns of the specimen at 5/1000 and the final stage are shown in Fig. 3. Under both positive and negative loadings, flexural cracks occurred by 2/1000 at the bottom of the specimen. After that, flexural cracks expanded upward and to the middle of the specimen. Shear cracks occurred at the cotter by 5/1000 and then extended. Under both positive and negative loadings, flexural shear cracks occurred by 5/1000. Under positive loading, the main bar at the compressive end yielded (yield strain 2146×10^{-6}) by 5/1000, and the main bar at the tensile end yielded by 15/1000. The corner area at the bottom appeared to crack vertically and crumbled slightly by 5/1000. At the final stage, the strength decreased due to shear failure of the cotters and crumbling at the bottom. The specimen maintained the axial load by the final cycle at 30/1000.

3.2 Load Deflection Curves

Figure 4 shows the load deflection curves. The maximum strength of positive loading was 103.0 kN at 15/1000, and that of negative loading was 107.5 kN at 7.5/1000, respectively. The strength decreased slightly after 20/1000 under positive loading and after 10/1000 under negative loading.

3.3 Strain Distribution of Hoop (Measuring Point in Thickness Direction)

3.3.1 Horizontal strain distribution

Figures 5 and 6 show the horizontal strain distribution of the hoop at heights of 42.5 and 152.5 mm, respectively. The strain was measured by strain gages attached to both sides of the hoop at the neutral axis, and the strain values are the average of both sides. The attachment position of strain gages at the hoop was the midpoint in the thickness direction of the specimen. The thickness direction is perpendicular to the loading direction, so the value of the measuring point in the thickness direction is considered to indicate the confinement effect of concrete on the vertical compressive stress rather than the shear reinforcing effect on the lateral force. The distribution was longitudinal in the cross section of the specimen, and at the peak of positive loading for each drift angle. The figures show the relationship between the strain of the hoop and the distance from the compressive end.

Strain increased with the increase in drift angle at all measuring points at both heights. At a height of

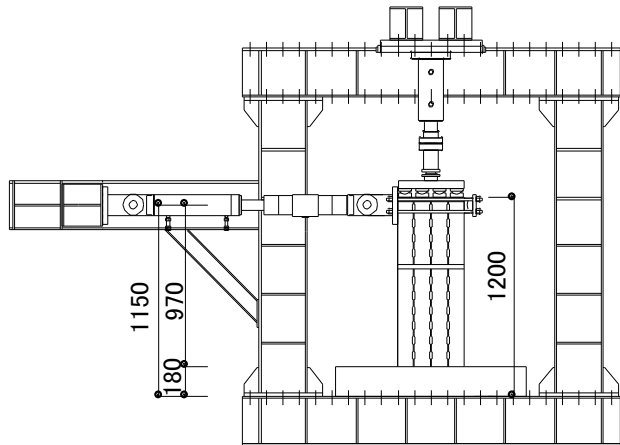


Fig. 2 Loading System

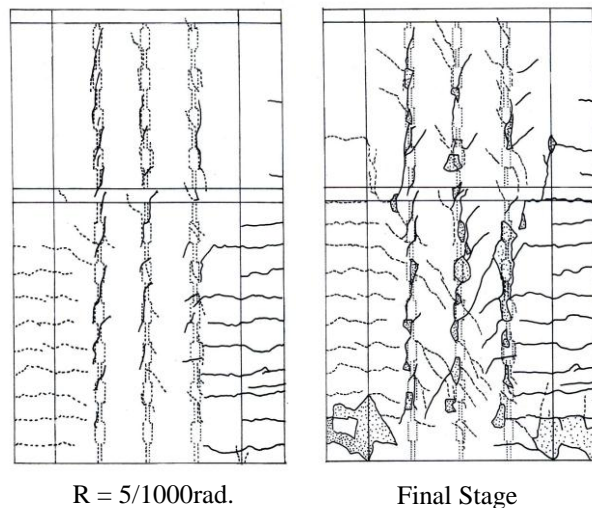


Fig. 3 Crack Patterns

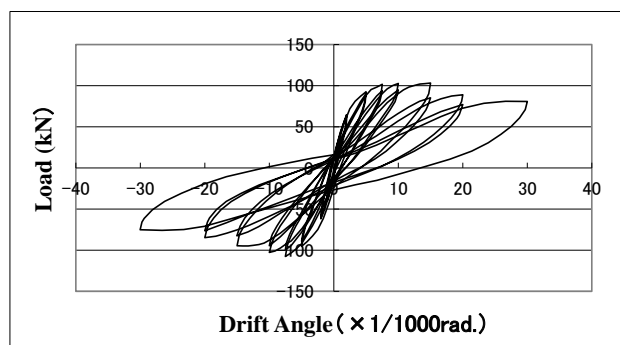


Fig. 4 Load - Deflection Curve

42.5 mm, the values at the point 9 mm from the compressive end were the largest, and the nearer the point was to the compressive end, the larger the value. The increase in strain at the points 114 and 187 mm from the compressive end with the increase in drift angle was small. At a height of 152.5 mm, the increase in strain at the point 114 mm from the compressive end was small up to 5/1000, but after 7.5/1000, the strain increased considerably. After 10/1000, the value of the point was the largest in the distribution. Comparing the heights, the increase in strain at the point 114 mm from the compressive end with the increase in drift angle was small at a height of 42.5 mm, and very large at a height of 152.5 mm.

3.3.2 Vertical strain distribution

Figure 7 shows the vertical strain distribution of the hoop at the measuring point 9 mm from the compressive end. The figure shows the relationship between the strain of the hoop and the height from the bottom at the peak of positive loading for each drift angle. Strain increased near the bottom as a whole. Up to 2/1000, the strain increased at an approximately constant rate toward the bottom. On the other hand, after 5/1000, the increment of strain near the bottom was remarkable at heights below 200 mm. During the fracture process mentioned above, the main bar at the compressive end yielded by 5/1000, and the corner area at the bottom appeared to crack vertically and crumbled slightly by 5/1000. From the fracture process and vertical strain distribution of the hoop, it is considered that the concrete at the compressive end was elastic at all heights up to 2/1000 and a range of approximately 200 mm at the bottom became plastic after 5/1000.

3.4 Strain Distribution of Horizontal Tied Rebars

Figures 8 and 9 show the strain distribution of the horizontal tied rebars at heights corresponding to the second and third floor level, respectively. At the second floor level, the strain increased remarkably at a drift angle of 2/1000 to 5/1000. The strain at the point 93 mm from the compressive end exceeded the yield strain and increased dramatically after 20/1000. At the third floor level, the strain increased remarkably at the points 202.5 mm and 255.5 mm from the compressive end after 20/1000.

3.5 Horizontal Distribution of Vertical Strain at the Bottom

3.5.1 Strain distribution measured by displacement transducers

Figure 10 shows the horizontal distribution of the vertical strain measured by displacement transducers.

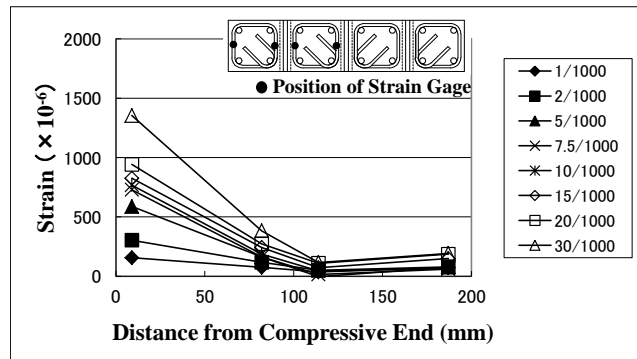


Fig. 5 Horizontal Strain Distribution of Hoop (Height of 42.5 mm)

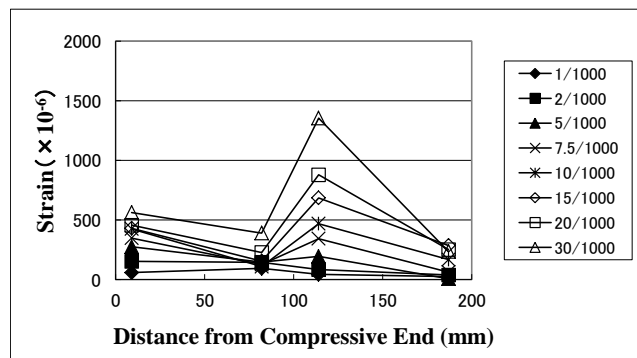


Fig. 6 Horizontal Strain Distribution of Hoop (Height of 152.5 mm)

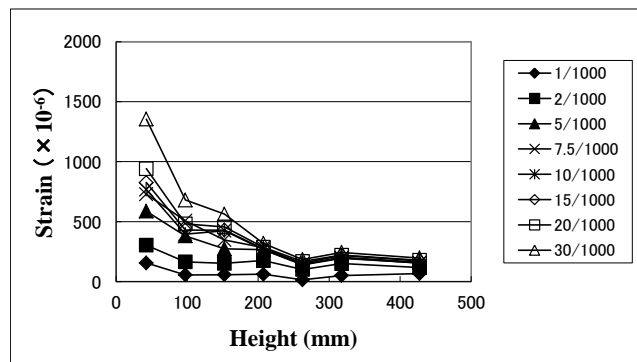


Fig. 7 Vertical Strain Distribution of Hoop

The measuring length was 65 mm. The figure shows the relationship between the vertical strain and the distance from the compressive end at the peak of positive loading for each drift angle. The strain changed from compressive to tensile between the compressive end and tensile end as a whole up to 5/1000. On the other hand, the tensile strain at the point 78 mm from the compressive end increased remarkably after 7.5/1000. That is, independent movement was observed at the bottom of the precast column at the compressive end.

3.5.2 Strain distribution of main bars measured by strain gages

Figure 11 shows the horizontal distribution of the main bars at a height of 25 mm from the bottom. The figure shows the relationship between the strain of the main bars and the distance from the compressive end at the peak of positive loading for each drift angle. The strain changed from compressive to tensile between the compressive end and tensile end as a whole up to 5/1000. On the other hand, the compressive strain at the point 72 mm from the compressive end began to decrease after 7.5/1000, and it changed to tensile strain at 15/1000. This corresponds to the tendency of the strain distribution measured by displacement transducers, and it is considered to be the independent movement at the bottom of the precast column at the compressive end.

3.6 Sliding and Opening in the Vertical Joint

3.6.1 Horizontal distribution of opening

Figures 12, 13 and 14 show the horizontal distribution of the opening in the vertical joint between the precast columns under positive loading. In the figure, the first, second and third array show the horizontal distribution at the lower part of the first story (height 170 mm), the upper part of the first story (height 415 mm) and the middle part of the second story (height 805 mm), respectively. The horizontal relative displacement between the precast columns was measured by the displacement transducer as the opening. The opening increased with the increase in the drift angle at any array.

At the first array, the increase in the opening was small up to 5/1000, but the opening

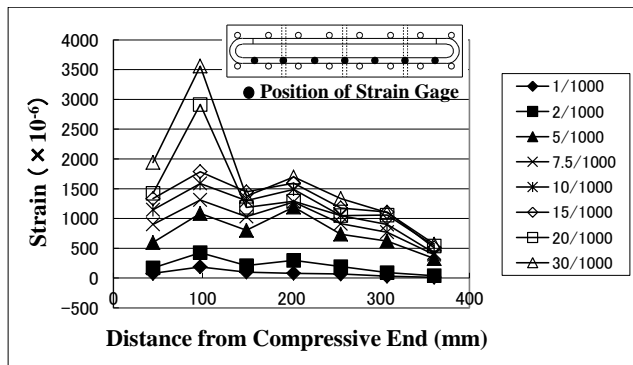


Fig. 8 Strain Distribution of Horizontal Tied Rebars (Second Floor Level)

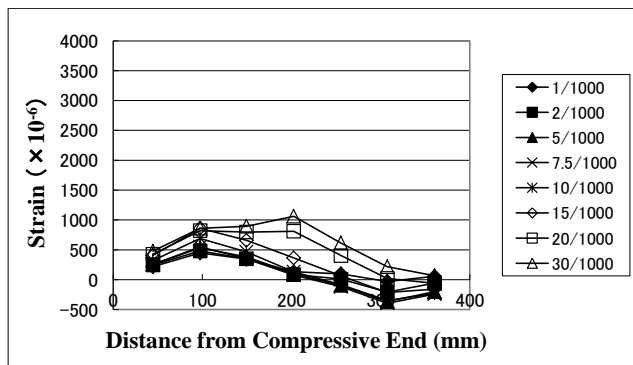


Fig. 9 Strain Distribution of Horizontal Tied Rebars (Third Floor Level)

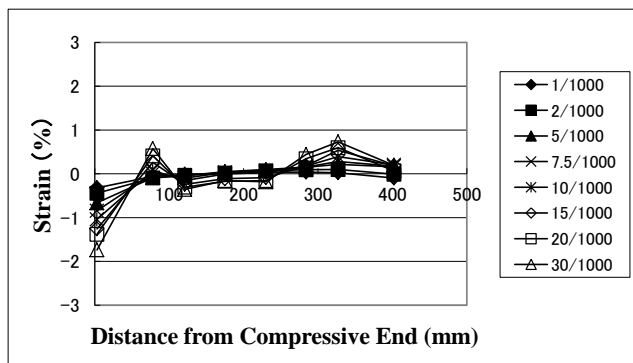


Fig. 10 Horizontal Distribution of Vertical Strain at Bottom Measured by Displacement Transducer

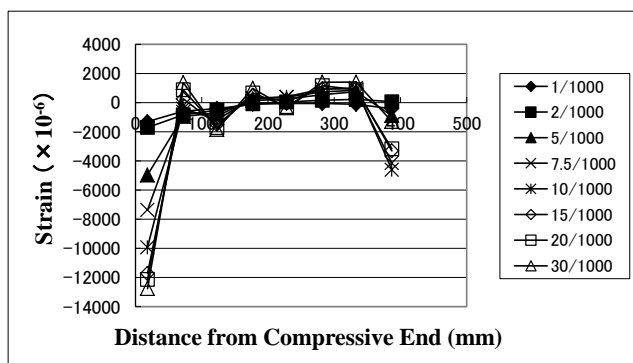


Fig. 11 Horizontal Strain Distribution of Main Bar at Bottom

increased greatly after 7.5/1000. Comparing in the horizontal direction, the opening was larger on the compression side. The largest opening was 2.4 mm in width on the compressive side at 30/1000. At the second array, the increase in the opening was small up to 2/1000, but the opening increased greatly after 5/1000. Comparing in the horizontal direction, the opening of both sides was larger than that of the midpoint. This tendency was remarkable after 7.5/1000. The distribution was approximately symmetric. The largest opening was 3.7 mm in width on the tensile side at 30/1000. At the third array, the opening increased at 10/1000 and 15/1000 compared with under 7.5/1000 on the compressive side, and did not increase after that. The opening increased after 15/1000 on the tensile side and at the midpoint. The opening of the midpoint was larger than that of both sides at 20/1000 and 30/1000. The largest opening was 1.0 mm in width at the midpoint at 30/1000.

Comparing the openings by the average value of each array, the following was revealed. The opening of the second array was largest and that of the first array was the second largest. With regard to the horizontal distribution of the opening, the opening on the compressive side was largest and decreased toward the tensile side at the first array. On the other hand, the openings on both sides were larger than that at the midpoint at the second array and the opening at the midpoint was largest at the third array at the final cycle of loading.

3.6.2 Horizontal distribution of sliding

Figures 15, 16 and 17 show the horizontal distribution of sliding at the vertical joint between the precast columns under positive loading. The measuring point of sliding corresponds to that of the opening mentioned above. The vertical relative displacement between the precast columns was measured by the displacement transducer as the sliding. Positive sliding was defined as the case of sliding up on the compressive side in the vertical joint under positive loading. The sliding increased with the increase in the drift angle at any array.

At the first array, the increase in the sliding was small up to 2/1000, but the sliding increased largely after 5/1000. Comparing in the horizontal direction, the sliding was larger on the compression side. This tendency corresponded to that of the opening measured at the first array. The largest sliding was 3.2 mm on the compressive side at 30/1000. At the second array, the increase in the sliding was small up to 2/1000, but the sliding increased largely after 5/1000 just like the sliding at the first array. Comparing in the horizontal direction, the sliding was larger on the compression side like at the first array. However, the increase in sliding with the increase in drift angle on the tensile side was larger than that of the first array. The tendency of being larger on the compressive side was different from that of

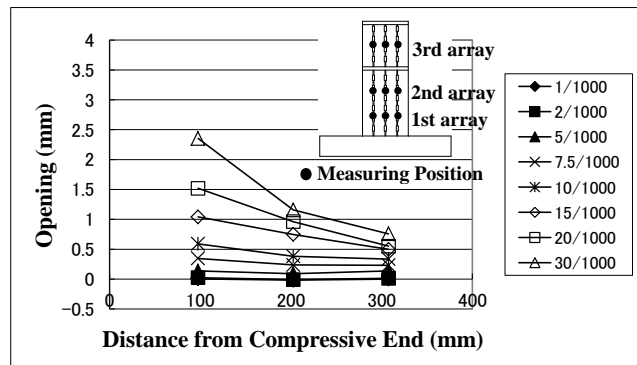


Fig. 12 Horizontal Distribution of Opening (First Array)

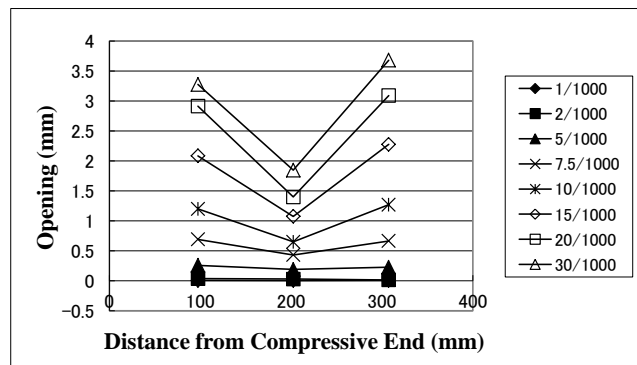


Fig. 13 Horizontal Distribution of Opening (Second Array)

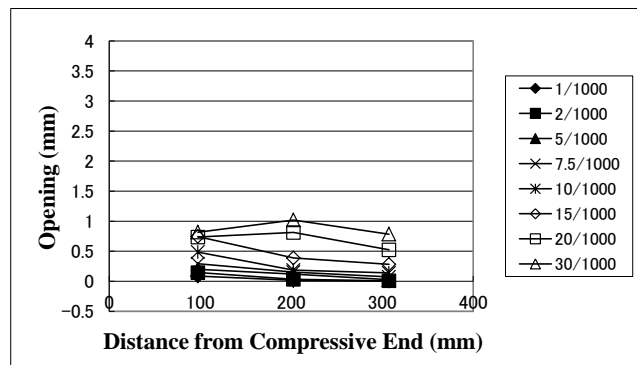


Fig. 14 Horizontal Distribution of Opening (Third Array)

the opening at the same measuring points, which was smallest at the midpoint. The largest sliding was 3.9 mm on the compressive side at 30/1000. At the third array, the sliding increased gradually up to 10/1000, and the increment of sliding increased after 15/1000. Comparing in the horizontal direction, the sliding was larger on the compression side, but the difference in sliding between the compression side and tensile side was smaller than that of the first and second array. The largest sliding was 1.4 mm on the compressive side at 30/1000.

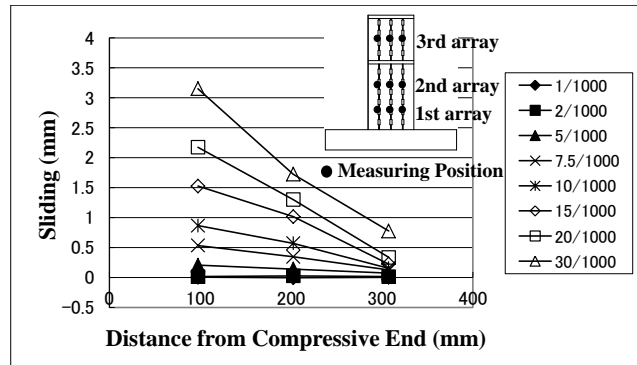


Fig. 15 Horizontal Distribution of Sliding (First Array)

Comparing the sliding by the average value of each array, the following was revealed. The sliding of the second array was largest and that of the first array was the second largest. This tendency corresponded to that of the opening. On the other hand, the sliding on the compressive side was largest at any array. This tendency was different from that of the opening. That is, in the case of the opening, the value at the midpoint was smallest at the second array and was largest at the third array.

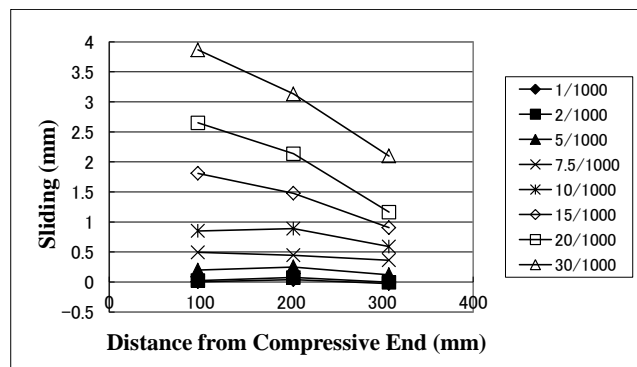


Fig. 16 Horizontal Distribution of Sliding (Second Array)

Comparing the distribution of the opening and sliding with the crack patterns of the specimen shown in Fig. 3, the following was revealed. In the crack patterns at both the first and second story at 5/1000, more shear cracks were observed at the vertical joint on the compressive side rather than the tensile side. This tendency of crack patterns corresponded to that of the horizontal sliding distribution at each array. In the final stage, the crumbling and the exfoliation of the grout in the vertical joint and the concrete around the cotter were observed most often at the upper part of the first story, and second most often at the lower part of the first story. This tendency of the fracture corresponded to that in the comparison of the average opening and sliding at each array.

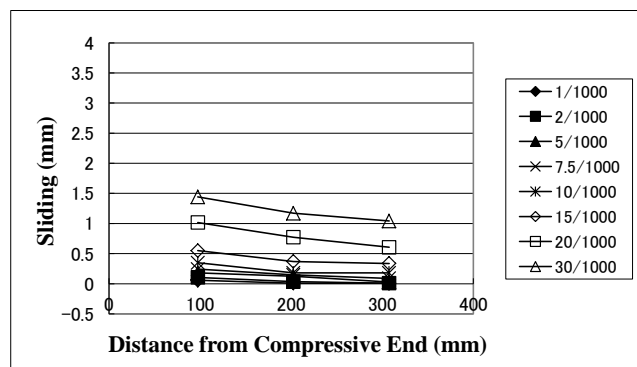


Fig. 17 Horizontal Distribution of Sliding (Third Array)

4. CONCLUSIONS

A lateral loading test on full precast wall columns simulating the area near the corner of an L-shaped core wall was conducted in order to examine the seismic performance. Major findings are as follows:

- (1) In the vertical strain distribution of the hoop, the increment of strain near the bottom was remarkable at a height below 200 mm after 5/1000. This area corresponded to the crumbling area in the fracture process. It is considered that a range of approximately 200 mm at the bottom became plastic after 5/1000.

(2) In the horizontal distribution of vertical strain at the bottom, the tensile strain at the point 78 mm from the compressive end increased remarkably after 7.5/1000. That is, independent movement was observed at the bottom of the precast column at the compressive end.

(3) Both the opening and sliding in the vertical joint were largest at the upper part of the first story. The largest values of opening and sliding were 3.7 mm and 3.9 mm, respectively. On the other hand, their horizontal distribution was different. The distribution of the opening was symmetric on the compressive side and the tensile side, and that of the sliding was larger on the compressive side.

ACKNOWLEDGEMENT

This work was supported by JSPS KAKENHI (23560683).

REFERENCES

- 1) Nakachi, T., Toda, T., and Tabata, K. (1996). Experimental study of deformation capacity of reinforced concrete core walls after flexural yielding. *Proceedings of the 11th World Conference on Earthquake Engineering*, Paper No. 1714.
- 2) Minami, N., Nakachi, T. (2008). Three-dimensional nonlinear finite element analysis on reinforced concrete walls enhanced by transverse confining steel. *Proceedings of the 14th World Conference on Earthquake Engineering*, Paper ID 14-0246.
- 3) Komiya, Y., Yamamoto, K. et al. (2003). Experimental study of R/C wall-columns with vertical joints between pre-cast and cast-in-place parts. *Summaries of Technical Papers of Annual Meeting of Architectural Institute of Japan*, 255-258.
- 4) Kuboyama, H., Nakazawa, H. et al. (2009). Seismic behavior of precast R/C corewalls of different strength. *Summaries of Technical Papers of Annual Meeting of Architectural Institute of Japan*, 463-468.